Acta Cryst. (1982). B**38**, 2793–2797

The Structure of the Linear Chain Tetraammineplatinum(II)-tetraamminedibromoplatinum(IV) Hydrogensulfate, $[Pt(NH_3)_4][PtBr_2(NH_3)_4](HSO_4)_4$

BY MASAKO TANAKA AND IKUJI TSUJIKAWA

Department of Chemistry, Faculty of Science, Kyoto University, Kyoto 606, *Japan*

AND KOSHIRO TORIUMI AND TASUKU ITO

Institute for Molecular Science, Okazaki National Research Institutes, Okazaki 444, *Japan*

(*Received* 12 *March* 1982; *accepted* 14 *June* 1982)

Abstract

The crystal structure of the title compound has been determined by single-crystal X-ray diffractometry at 269 K. The crystal data are monoclinic, $P2_1/a$, a = 10·654 (1), b = 10·282 (1), c = 5·505 (1) Å, β = 93·17 (1)°, U = 602·1 (2) Å^3, Z = 2, D_x = 2·95 Mg m^{-3}, and μ(Mo $K\alpha$) = 16·14 mm^{-1}. Final R = 0·029 for 1448 independent reflections. This compound contains linear chains comprising alternately arranged octahedral $[PtBr_2(NH_3)_4]^{2+}$ and square-planar $[Pt(NH_3)_4]^{2+}$ units along the c axis, in which the Pt—Br distances are 2·476 (1) and 3·029 (2) Å. The crystal shows statistical disorder of the Br positions.

Introduction

For a decade, the chemistry and physics of one-dimensional compounds have aroused interest (Keller, 1977; Toombs, 1978; Devreese, 1979, and references therein). Among such compounds containing transition metals, KCP $\{K_2[Pt(CN)_4]Br_{0.3}.3H_2O\}$ and related compounds which have direct interactions between platinum ions have been studied extensively. They show metallic behavior at high temperature and become semiconductive at low temperature, where the Kohn anomaly and the Peierls distortion characteristic of one-dimensional compounds are observed. Meanwhile, Wolffram's red salt and its analogues have been synthesized and studied (Endres, Keller, Martin & Traeger, 1979; Matsumoto, Yamashita, Kida & Ueda, 1979; Endres, Keller, Martin, Traeger & Novotny, 1980). They contain linear chains of halide-bridged platinum ions in the two different oxidation states Pt^{II} and Pt^{IV}. These compounds show a considerable interaction between platinum ions in each chain through bridging halide ions. They also show interesting physical properties: semiconductive behavior with a conductivity of $10^{-8} \sim 10^{-12}$ Ω^{-1} cm^{-1} at room temperature and a strong absorption in the visible region (Yamada & Tsuchida, 1956; Day, 1975). Their conductivity increases by a factor of 10^3 or more under a pressure of about 10^8 Pa (Thomas & Underhill, 1971; Hamaue, Aoki, Yamashita & Kida, 1981). Thus, the physical properties including the mechanism of conduction should be very interesting.

So far, Wolffram's red salt analogues with ethylamine, ethylenediamine (en), propylenediamine (pn), or trimethylenediamine (tn) as ligands, halide ions as bridging ligands and halide ions, BF_4^- or ClO_4^- as counter ions, have been synthesized. Recently, compounds that contain the simplest amine, NH_3, as ligands of the Pt atoms have been synthesized (Layek & Papavassiliou, 1981) but their crystal structures have not yet been determined. Exclusion of steric hindrance and a highly symmetric environment about the Pt atoms may influence the conductivity. The small NH_3 ligand may reduce the steric repulsion between the Pt^{IV} and Pt^{II} complexes, resulting in a shorter Pt—Pt separation. Moreover, since every Pt atom is coordinated by the same NH_3 ligand, a distinction between the oxidation states of the Pt atoms is impossible, at least in relation to the geometry around the Pt atoms. In this paper the synthesis and crystal structure of the compound containing NH_3 ligands are reported.

Experimental

The title complex was prepared from the Magnus green salt analogue $[Pt(NH_3)_4][PtBr_4]$ by reaction with appropriate oxidants, such as Br_2, $KBrO_3$, H_2O_2 and $Na_2S_2O_3$, in 62% sulfuric acid. The Magnus green salt analogue, which is green, turned greenish brown through the action of oxidant, and then the solution and the precipitates were left untouched at room tem-

0567-7408/82/112793-05$01.00

perature for several weeks. Consequently lustrous green needles crystallized along with powdered precipitates. Single crystals were grown by recrystallization from 62% sulfuric acid below 293 K, since twinning is frequently observed at a higher temperature. The crystal decomposed above 335 K. Analysis: calculated for $[Pt(NH_3)_4][PtBr_2(NH_3)_4](HSO_4)_4$: Pt 36·31, Br 14·87, S 11·94, O 23·82, N 10·43, H 2·63; found: Pt 34·45, Br 14·46, S 12·11, O 23·53, N 10·59, H 2·64%.

The crystals are dark brown and light yellow for light polarized parallel and perpendicular to the needle axis, respectively.

Preliminary oscillation and Weissenberg photographs (Cu $K\alpha$ radiation) about the needle axis showed that it corresponds to the c axis and the crystal is pseudo-tetragonal. It was also shown that crystals grown at a temperature higher than 293 K are frequently twinned. Two individuals, 1 and 2, in the twinned crystal are related to each other as follows: $c(1) = \pm c(2)$ and $\pm a^*(1) + b^*(1) = a^*(2) + b^*(2)$. Neither diffuse scattering nor Bragg reflections corresponding to a superstructure were observed on the photographs.

A crystal with dimensions 0·38 × 0·22 × 0·10 mm coated with a thin layer of paraffin was used for the intensity measurements. Intensity data were collected with graphite-monochromatized Mo $K\alpha$ radiation on a Rigaku AFC-5 four-circle diffractometer equipped with a variable-temperature apparatus using a cold nitrogen-gas stream. The measurement was carried out at 269 K, because the peak profile for each Bragg spot is broadened considerably at lower temperatures. Within the range $2\theta \leq 60°$, 1448 independent reflections with $|F_o| \geq 3\sigma(|F_o|)$ were obtained. The intensities were corrected for Lorentz and polarization factors and for absorption.

The positions of the Pt and Br atoms were determined from the Patterson maps. The Br atoms were disordered on two possible sites near the center of symmetry $(0,0,\frac{1}{2})$. From successive Fourier syntheses, positions of the nonhydrogen atoms could be determined. Block-diagonal least-squares calculations were carried out with anisotropic thermal parameters and the R value converged to 0·033. All the H-atom positions were identified in the subsequent difference-Fourier maps. At the final stage, block-diagonal least-squares calculations with anisotropic thermal parameters for non-hydrogen atoms and isotropic thermal parameters for H atoms were carried out. The scattering factors and anomalous-scattering corrections for non-hydrogen atoms were taken from *International Tables for X-ray Crystallography* (1974). For H atoms, the values given by Stewart, Davidson & Simpson (1965) were used. The weighting scheme employed was $w = [\sigma^2_{count} + (0{\cdot}015F_o)^2]^{-1}$. The final R value was 0·029 for 1448 independent reflections. The atomic parameters are listed in Table 1.*

The temperature dependence of the lattice parameters from 233 to 292 K was also measured on the diffractometer, based on 50 reflections with $25° \leq 2\theta \leq 30°$. Broadening of the Bragg spots was observed at lower temperatures and the change of behavior of the Bragg spots was reversible.

Table 1. *Final atomic parameters* ($\times 10^4$, *for* H $\times 10^3$) *and thermal parameters*

	x	y	z	B_{eq}* or B (Å^2)
Pt	0	0	0	1·3
Br(1)	15 (2)	40 (2)	4499 (3)	2·0
S(1)	1436 (1)	3622 (2)	4642 (3)	1·7
N(1)	−533 (6)	1916 (5)	−335 (10)	2·0
N(2)	1860 (5)	560 (6)	123 (10)	1·9
O(1)	1703 (7)	5106 (5)	4379 (17)	3·2
O(2)	2140 (5)	3009 (6)	2801 (10)	3·0
O(3)	1783 (6)	3263 (6)	7104 (9)	3·4
O(4)	69 (5)	3443 (6)	4102 (12)	3·1
H(N1)1	−115 (8)	209 (8)	−143 (14)	3·0 (1·7)
H(N1)2	2 (9)	229 (9)	−120 (19)	5·3 (2·3)
H(N1)3	−49 (9)	238 (10)	137 (18)	7·0 (2·7)
H(N2)1	219 (8)	78 (9)	−197 (15)	4·5 (2·1)
H(N2)2	206 (8)	131 (9)	140 (15)	4·3 (2·1)
H(N2)3	248 (12)	5 (6)	67 (24)	3·2 (2·8)
H(O1)1	92 (9)	560 (11)	500 (17)	4·6 (2·2)

* The equivalent isotropic temperature factor is calculated using the expression $B_{eq} = \frac{4}{3}\sum_i \sum_j \mathbf{a}_i.\mathbf{a}_j \beta_{ij}$, where the $\mathbf{a}_i$'s are the unit-cell edges in direct space.

Description of the structure

A stereoscopic view of the crystal structure is shown in Fig. 1. Bond lengths and bond angles are listed in Table 2. The Pt atom is coordinated in a plane by four N atoms of the ligands with an average Pt—N distance of 2·059 (6) Å. As shown in Fig. 2 the complex units are stacked in the **c** direction, along which the Pt and Br atoms alternate. The Br atoms occupy each of two positions near the center of symmetry $(0,0,\frac{1}{2})$ with a probability of $\frac{1}{2}$, these positions being 0·560 (2) Å apart. Because of the disorder in the arrangement of the Br atom, the oxidation states of the Pt atoms cannot be identified. The two Pt—Br distances are 3·029 (2) and 2·476 (1) Å. The shorter distance corresponds to the distance between the Pt^{IV} and Br atoms, and the longer between the Pt^{II} and Br atoms.

The hydrogensulfate ions are located in the channels among the chains. Two adjacent hydrogensulfate ions,

* List of anisotropic thermal parameters for non-hydrogen atoms and structure factors have been deposited with the British Library Lending Division as Supplementary Publication No. SUP 36998 (11 pp.). Copies may be obtained through The Executive Secretary, International Union of Crystallography, 5 Abbey Square, Chester CH1 2HU, England.

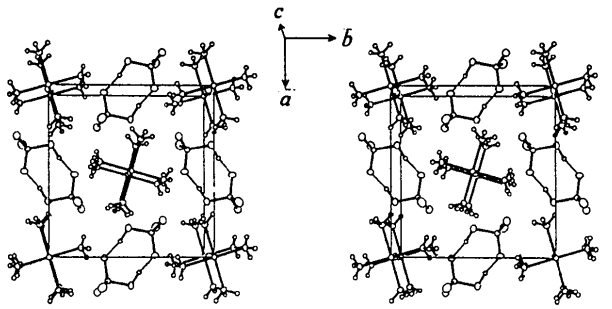

Fig. 1. Stereoscopic drawing of the crystal structure along the *c* axis.

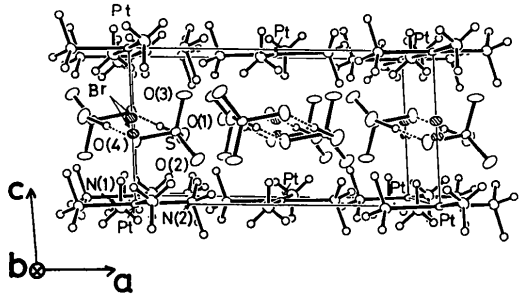

Fig. 2. Perspective drawing of the crystal structure along the *b* axis.

Table 2. *Bond distances* (Å) *and angles* (°) *with their estimated standard deviations* (*in parentheses*)

Pt–Br(1)	2·476 (1)	Br(1)–Pt–N(1)	93·5 (2)
Pt–N(1)	2·056 (6)	Br(1)–Pt–N(2)	90·5 (2)
Pt–N(2)	2·061 (6)	N(1)–Pt–N(2)	89·8 (2)
S(1)–O(1)	1·560 (5)	O(1)–S(1)–O(2)	105·0 (4)
S(1)–O(2)	1·439 (6)	O(1)–S(1)–O(3)	107·5 (4)
S(1)–O(3)	1·434 (5)	O(1)–S(1)–O(4)	106·6 (4)
S(1)–O(4)	1·482 (5)	O(2)–S(1)–O(3)	115·8 (4)
		O(2)–S(1)–O(4)	110·4 (4)
		O(3)–S(1)–O(4)	110·9 (4)

which are related by a center of symmetry, are dimerized by strong hydrogen bonds O(1)–H···O(4) [2·582 (9) Å] to form an octagonal ring consisting of $(O–S–O–H\cdots)_2$. The location of the H atom taking part in the hydrogen-bond formation was clearly revealed in the difference-Fourier maps. The distances between the N atoms of the ligands and the O atoms of the counter ions HSO_4^- are shown in Table 3. The hydrogen-bond schemes involving N(1) and N(2) are apparently different, as shown in Fig. 3. There are five independent hydrogen bonds to N atoms, forming a three-dimensional network. The details of the hydrogen-bond network are different in the **a** and **b** directions. Two hydrogen bonds [N(1)···O(3) 3·122 (8), N(1)···O(2) 3·099 (8) Å] are almost parallel to the *a* axis, and one hydrogen bond [N(2)···O(2) 2·925 (8) Å] is parallel to the *b* axis. The directions of

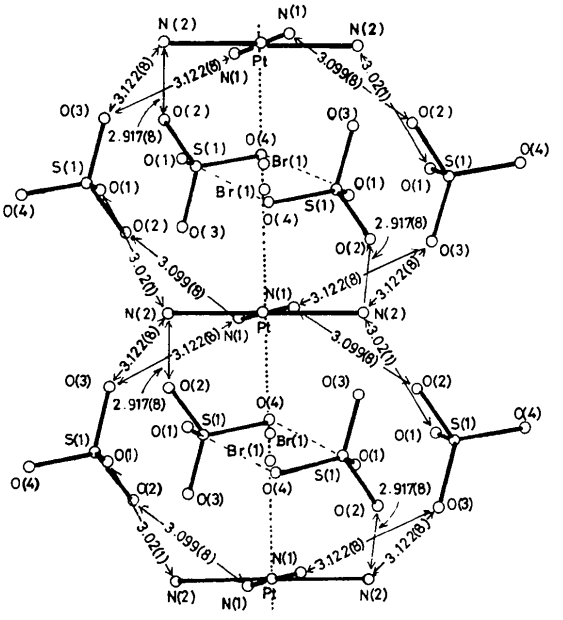

Fig. 3. A perspective drawing of the the –Pt–Br···Pt··· chain. Hydrogen bonds between the O atoms of HSO_4^- and the N atoms of the ligand are indicated by the solid lines, and hydrogen bonds between HSO_4^- are indicated by broken lines [2·582 (9) Å]. The circles indicate the center of the atom positions.

Table 3. *Hydrogen-bond distances* (Å) *with their estimated standard deviations*

Key to symmetry operations: (i) $-x, 1-y, 1-z$; (ii) $\frac{1}{2}+x, \frac{1}{2}-y, z$; (iii) $\frac{1}{2}+x, \frac{1}{2}-y, 1+z$; (iv) $\frac{1}{2}-x, -\frac{1}{2}+y, -z$; (v) $\frac{1}{2}-x, -\frac{1}{2}+y, 1-z$.

D–H···*A*	*D*···*A*	H···*A*
O(1)–H(O1)1···O(4^{i})	2·582 (9)	1·54 (10)
N(1)–H(N1)1···O(3^{ii})	3·122 (8)	2·33 (8)
N(1)–H(N1)3···O(2^{iii})	3·099 (8)	2·71 (10)
N(2)–H(N2)1···O(1^{iv})	3·020 (11)	1·95 (9)
N(2)–H(N2)2···O(2)	2·925 (8)	1·91 (9)
N(2)–H(N2)3···O(3^{v})	3·122 (8)	2·32 (9)

the remaining two hydrogen bonds roughly correspond to [110]. Thus hydrogen bonding may be weaker in the **b** direction than in the **a**. Br atoms are not involved in any hydrogen bonding.

Discussion

Wolffram's red salt analogues, hitherto studied by X-ray measurements (Craven & Hall, 1961; Brown & Hall, 1976; Breer, Endres, Keller & Martin, 1978; Matsumoto, Yamashita, Kida & Ueda, 1979), often show one-dimensional superstructures along the –Pt–*X*···Pt··· chains with a repeat distance of two

Pt–Pt separations, but most of them show no correlation between the positions of Pt^{II} or Pt^{IV} in neighboring chains. Thus, a repeat distance of one Pt–Pt separation is found on average for the three-dimensional structure, but the one-dimensional superstructure still appears as diffuse scattering between the reciprocal-lattice planes of the structure with averaged valency. On the other hand, in Wolffram's red salt analogues, $[Pt(pn)_2][PtBr_2(pn)_2](ClO_4)_4$, $[Pt(tn)_2][PtCl_2(tn)_2](BF_4)_4$, $[Pt(tn)_2][PtBr_2(tn)_2](BF_4)_4$, and $[Pt(tn)_2][PtBr_2(tn)_2](ClO_4)_4$, two Pt–Pt separations are observed for the three-dimensional structure (Endres, Keller, Martin, Traeger & Novotny, 1980; Matsumoto, Yamashita & Kida, 1978).

In contrast to the above, in $[Pt(NH_3)_4][PtBr_2(NH_3)_4](HSO_4)_4$ neither diffuse scattering nor Bragg reflections corresponding to the structure having a repeat distance of two Pt–Pt separations are observed, but a repeat distance of one Pt–Pt separation is found for the three-dimensional structure. This is the same as in $[Pt(pn)_2][PtI_2(pn)_2]I_4$ (Endres, Keller, Martin, Traeger & Novotny, 1980).

Two explanations are possible: One chain is formed by many fine filament fragments consisting of $-Pt-Br\cdots Pt\cdots$ stacks and then no correlation exists between neighboring chains, so that the periodicity of two Pt–Pt separations does not develop sufficiently to produce diffuse scattering or Bragg reflections. Another possibility is as follows. Since the difference between Pt^{II} and Pt^{IV} sites is only determined by the Br^- ion location, Pt^{II} and Pt^{IV} may be interchanged through the motion of the Br^- ion between two possible sites, 0·560 (2) Å apart. If the rate of interchange is faster than the X-ray-scattering time scale, only the average structure will appear. The latter explanation is doubtful in view of the mass of the Br atom and the former is more likely.

The differences between the $Pt^{II}\cdots X$ and $Pt^{IV}-X$ distances are very interesting in Wolffram's red salt analogues because their electrical conductivities should be very sensitive to the distances. In these compounds the oxidation states of the Pt atoms are not strictly divalent or tetravalent due to the interaction between the Pt atoms through the bridging halide ion. If X is located midway between the Pt atoms, every Pt atom becomes equivalent, that is trivalent, and the compound is thought to be metallic. In Wolffram's red salt analogues, the counter ions are considered to play a role in the formation of one-dimensional chains consisting of Pt and halogen atoms. This may involve hydrogen bonds between ligands and counter ions which may draw electrons from the Pt atoms to reduce the $Pt^{II}\cdots X$ repulsive force and link closely the Pt^{II} and Pt^{IV} units. In addition to hydrogen bonds, we must consider the steric and symmetry effects of ligands as factors determining Pt–Pt separations.

In this compound, the exclusion of the steric hindrance and highly symmetric environments about the Pt atoms are realized by introducing the simplest amine, NH_3, as the ligand, but in contrast to other Wolffram's red salt analogues the counter ions HSO_4^- form strong hydrogen bonds between themselves and as a result the hydrogen bond required to link the Pt^{II} and Pt^{IV} units closely may be weakened. Consequently the difference between the $Pt^{II}\cdots X$ and $Pt^{IV}-X$ distances may not be reduced.

The $Pt^{II}\cdots X$ and $Pt^{IV}-X$ distances and their differences for compounds with X = Br are listed, together with the Pt–Pt separations, in Table 4. Generally speaking, the shorter the Pt–Pt separation, the smaller the difference between the $Pt^{II}\cdots Br$ and $Pt^{IV}-Br$ distances. The compound containing Cu_3Br_5 as counter ions is exceptional, since it also contains halide-bridged copper chains (Endres *et al.*, 1979; Bekaroglu, Breer, Endres, Keller & Nam Gung, 1977). In comparison with the compound containing unidentate ligands $C_2H_5NH_2$, $[Pt(NH_3)_4][PtBr_2(NH_3)_4](HSO_4)_4$ has about the same $Pt^{IV}-Br$ and shorter $Pt^{II}\cdots Br$ distances, which means that the difference in the oxidation states between Pt^{II} and Pt^{IV} becomes less. This is due to the exclusion of steric hindrance and the highly symmetric environment about the Pt atoms which surpass the effect of the hydrogen bonds in the dimeric counter ions. But this is not the case when this

Table 4. *The two distances between* Pt *and* Br *atoms together with their difference and* Pt–Pt *separation in* Å *in Wolffram's red salt analogues*

Amine	Counter ion	$Pt^{IV}-Br$ distance	$Pt^{II}\cdots Br$ distance	Difference	Pt–Pt separation	Reference
$(tn)_2$	BF_4	2·541	2·921	0·38	5·462	*a*
$(en)_2$	ClO_4	2·71	2·76	0·05	5·491	*b*
$(tn)_2$	ClO_4	2·546	2·955	0·409	5·501	*c*
$(NH_3)_4$	HSO_4	2·476 (1)	3·029 (2)	0·560 (2)	5·505 (1)	*d*
$(C_2H_5NH_2)_4$	Br	2·479	3·139	0·66	5·586	*e*
$(pn)_2$	Cu_3Br_5	2·55	3·07	0·52	5·617	*f*

References: (*a*) Matsumoto, Yamashita & Kida (1978). (*b*) Endres, Keller, Martin, Traeger & Novotny (1980). (*c*) Matsumoto, Yamashita & Kida (1978). (*d*) Present work. (*e*) Brown & Hall (1976). (*f*) Keller, Martin & Traeger (1978).

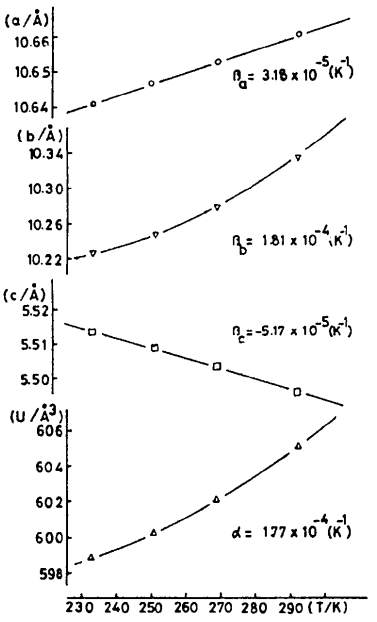

Fig. 4. Temperature dependence of lattice parameters. α and β are the coefficients of cubic and linear expansion, respectively.

compound is compared with compounds coordinated by the chelate ligands on which hydrogen bonds between ligands and counter ions may have more influence.

The complex cations and hydrogensulfate ions form a three-dimensional network of hydrogen bonds, as shown in Fig. 3. The —Pt—Br···Pt··· chains along **c** are linked by weak hydrogen bonds between the Pt complexes and the hydrogensulfate ions, loosely held together. This may give rise to stacking faults among the chains along **c**. As shown in Fig. 1, the packing modes of the complex and hydrogensulfate ions along **a** and **b** closely resemble each other. The twinning of this crystal may be interpreted in terms of the similarity of atomic arrangements along **a** and **b**.

The temperature dependence of the lattice constants is shown in Fig. 4. It can be seen that (i) the thermal expansion coefficient of the *b* axis is larger by an order than that of the *a* axis, and (ii) that of the *c* axis has a negative sign. The larger thermal expansion coefficient of the *b* axis is easily explained considering the difference between the hydrogen-bonding strengths along **a** and **b**. What contributes to the negative thermal expansion coefficient of the *c* axis is not clear, but lattice binding energy may be increased by increasing the *c* lattice constant at lower temperatures.

The calculations were carried out on the HITAC M-200 computer at the Computer Center of the Institute for Molecular Science with the *Universal Crystallographic Computation Program System UNICS* III (Sakurai & Kobayashi, 1979). This work was supported by the Joint Studies Program of the Institute for Molecular Science.

References

BEKAROGLU, O., BREER, H., ENDRES, H., KELLER, H. J. & NAM GUNG, H. (1977). *Inorg. Chim. Acta*, **21**, 183–186.

BREER, H., ENDRES, H., KELLER, H. J. & MARTIN, R. (1978). *Acta Cryst.* B**34**, 2295–2297.

BROWN, K. L. & HALL, D. (1976). *Acta Cryst.* B**32**, 279–281.

CRAVEN, B. M. & HALL, D. (1961). *Acta Cryst.* **14**, 475–480.

DAY, P. (1975). *Low-Dimensional Cooperative Phenomena*, edited by H. J. KELLER, pp. 191–214. New York: Plenum.

DEVREESE, J. T. (1979). *Highly Conducting One-Dimensional Solids*. New York: Plenum.

ENDRES, H., KELLER, H. J., MARTIN, R. & TRAEGER, U. (1979). *Acta Cryst.* B**35**, 2880–2882.

ENDRES, H., KELLER, H. J., MARTIN, R., TRAEGER, U. & NOVOTNY, M. (1980). *Acta Cryst.* B**36**, 35–39.

HAMAUE, Y., AOKI, R., YAMASHITA, M. & KIDA, S. (1981). *Inorg. Chim. Acta*, **54**, L12–L14.

International Tables for X-ray Crystallography (1974). Vol. IV. Birmingham: Kynoch Press.

KELLER, H. J. (1977). *Chemistry and Physics of One-Dimensional Metals*. NATO-ASI-Series B25. New York: Plenum.

KELLER, H. J., MARTIN, R. & TRAEGER, U. (1978). *Z. Naturforsch. Teil B*, **33**, 1263–1266.

LAYEK, D. & PAPAVASSILIOU, G. C. (1981). *Z. Naturforsch. Teil B*, **36**, 83–86.

MATSUMOTO, M., YAMASHITA, M. & KIDA, S. (1978). *Bull. Chem. Soc. Jpn*, **51**, 3514–3518.

MATSUMOTO, M., YAMASHITA, M., KIDA, S. & UEDA, I. (1979). *Acta Cryst.* B**35**, 1458–1460.

SAKURAI, T. & KOBAYASHI, K. (1979). *Rikagaku Kenkyusho Hokoku*, **55**, 69–77 (in Japanese).

STEWART, R. F., DAVIDSON, E. R. & SIMPSON, W. T. (1965). *J. Chem. Phys.* **42**, 3175–3187.

THOMAS, T. W. & UNDERHILL, A. E. (1971). *J. Chem. Soc. A*, pp. 512–515.

TOOMBS, G. A. (1978). *Phys. Rep.* C**40**, 181–240.

YAMADA, S. & TSUCHIDA, R. (1956). *Bull. Chem. Soc. Jpn*, **29**, 894–898.